

19 - EXPERIMENTAL METHOD TREE

Spacer v.1

ASTEROMORPH, INC.

HYPOTHESIS

This experimental design tests whether controlled injection of non-Gaussian noise into calcium signaling pathways via aperiodic modulation of extracellular calcium concentrations can restore oscillatory coherence in hepatocellular carcinoma (HCC) cells through stochastic resonance mechanisms, thereby re-engaging calcium-dependent cell cycle checkpoint regulation disrupted in malignancy. The rationale is based on observed disruptions in calcium homeostasis and oscillations in HCC cells compared to normal hepatocytes, with noise injection potentially enhancing signal coherence to suppress malignant proliferation selectively.

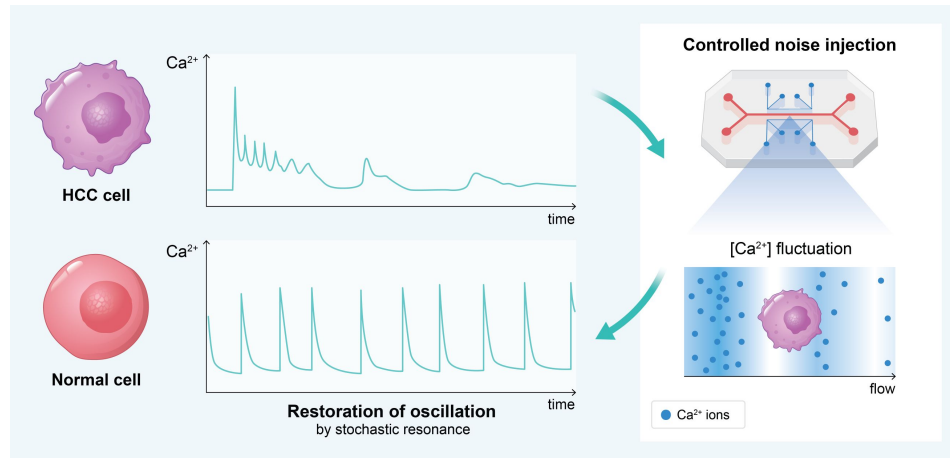


Figure 1: Hepatocellular carcinoma cells exhibit disrupted calcium oscillations. Controlled noise injection as extracellular calcium fluctuation could restore oscillatory coherence toward normal state, suppressing malignant phenotype.

1 STEP 1: CHARACTERIZE BASELINE CALCIUM OSCILLATION PATTERNS IN NORMAL AND HCC HEPATOCYTES.

1.1 APPROACH

Rationale. Establishing baseline differences in calcium signaling dynamics between normal and HCC cells is essential to confirm the hypothesis foundation, as disrupted oscillations in cancer cells are a prerequisite for testing restoration via noise. This step uses live-cell imaging, a feasible and established technique, to quantify oscillation frequency, amplitude, and coherence, addressing whether HCC cells exhibit less coherent patterns than normal cells.

Procedure.

1. Seed primary human hepatocytes (normal) and HepG2 HCC cells at 5×10^4 cells/well in 96-well plates coated with collagen I, culture in DMEM with 10% FBS at 37°C, 5% CO₂ for 24h.
2. Load cells with 5μM Fluo-4 AM calcium indicator dye for 30 min at 37°C, wash twice with HBSS (1.25 mM CaCl₂).

3. Perform live-cell confocal microscopy using a spinning-disk system at 37°C, acquiring images every 5s for 30 min to capture spontaneous oscillations.
4. Stimulate with 100 nM ATP to induce oscillations if spontaneous activity is low.
5. Analyze traces using ImageJ: quantify oscillation frequency (peaks/min), amplitude (fold-change from baseline), and coherence (autocorrelation decay time constant, τ ; lower τ indicates less coherence).
6. Include negative control (dye only, no cells) and positive control (ionomycin 1 μ M for maximal calcium response). Replicate in 3 independent experiments ($n = 50$ cells/group), analyze with unpaired t -tests ($p < 0.05$).

Required Resources.

- **Cell lines/models:** Primary human hepatocytes (e.g., from Lonza) for normal physiology; HepG2 cells (ATCC) as HCC model, chosen for their well-characterized calcium dysregulation.
- **Key reagents:** Fluo-4 AM (Invitrogen, 5 μ M); ATP (Sigma, 100 nM); Ionomycin (Sigma, 1 μ M); HBSS with 1.25 mM CaCl_2 .
- **Equipment:** Spinning-disk confocal microscope (e.g., PerkinElmer UltraVIEW); 96-well plates; ImageJ software for analysis.

1.2 EXPECTED OUTCOMES

- Normal hepatocytes show coherent oscillations ($\tau > 10$ min, frequency 0.1–0.5 Hz, amplitude 2–5 fold).
- HCC cells show disrupted patterns ($\tau < 5$ min, irregular frequency, sustained high baseline).
- No differences between cell types (null result).
- Technical artifacts (e.g., photobleaching leading to apparent low coherence).

1.3 MOST PROBABLE OUTCOME

HCC cells exhibit disrupted oscillations with lower coherence ($\tau \sim 2\text{--}4$ min) and higher baseline calcium compared to normal hepatocytes ($\tau \sim 15$ min), based on established literature showing altered calcium homeostasis in cancer cells due to pump dysregulation. However, complete absence of oscillations is unlikely, as HCC cells retain some responsiveness, potentially yielding partial differences rather than stark contrasts.

1.4 BRANCH 1.1: VALIDATE CALCIUM DYSREGULATION MECHANISMS

Trigger. Confirmation of disrupted oscillations in HCC cells (lower τ and irregular patterns).

Approach. Assess expression and function of key calcium regulators.

1. Perform qRT-PCR on RNA from both cell types using primers for PMCA1/4 (plasma membrane Ca^{2+} -ATPase), TRPV channels, and housekeeping gene GAPDH; normalize to normal cells.
2. Western blot for PMCA proteins using anti-PMCA antibodies (Abcam, 1:1000 dilution, with β -actin loading control).
3. Functional assay: Treat cells with PMCA inhibitor carboxyeosin (10 μ M) and repeat calcium imaging to confirm exacerbation of dysregulation.
4. Analyze with ANOVA, $n = 3$ replicates.

Resources. qRT-PCR kit (Qiagen); anti-PMCA antibodies (Abcam); carboxyeosin (Sigma, 10 μ M); immunoblotting system.

Expected Outcomes. Lower PMCA expression/function in HCC; no differences; unexpected up-regulation.

Most Probable. Modest downregulation of PMCA in HCC ($\sim 50\%$ reduction), consistent with known cancer adaptations for sustained signaling, but not complete loss, as cells maintain viability.

2 STEP 2: IMPLEMENT CONTROLLED NOISE INJECTION AND ASSESS OSCILLATION COHERENCE RESTORATION

2.1 APPROACH

Rationale. This core step tests the stochastic resonance hypothesis by introducing non-Gaussian noise via microfluidic modulation of extracellular calcium, measuring whether it enhances coherence in HCC cells without affecting normal cells. We use established microfluidic and imaging techniques for precise control and quantification.

Procedure.

1. Fabricate a microfluidic device with perfusion channels (e.g., using soft lithography with PDMS) for rapid solution switching.
2. Seed HepG2 and normal hepatocytes in device chambers; load with Fluo-4 AM as in Step 1.
3. Perfuse with HBSS at 1.25 mM CaCl_2 baseline, then apply aperiodic modulation: switch to 0.8 mM CaCl_2 for pulse durations of 1–5 s at frequencies 0.05–1 Hz, using Poisson-distributed intervals for non-Gaussian noise (controlled via syringe pump with LabVIEW software); total exposure 30 min.
4. Image cells simultaneously with confocal microscopy, acquiring every 5s.
5. Analyze coherence (τ from autocorrelation) pre- and post-modulation; compare to constant 1.25 mM control and Gaussian noise control (regular pulses).
6. Replicate $n = 3$ experiments, 30 cells/group, use paired t -tests.

Required Resources.

- **Cell lines/models:** Same as Step 1, for direct comparison.
- **Key reagents:** Fluo-4 AM; HBSS with varying CaCl_2 (0.8–1.25 mM).
- **Equipment:** Microfluidic fabrication setup (PDMS, Sylgard); syringe pump (Harvard Apparatus); LabVIEW software for modulation; confocal microscope.

2.2 EXPECTED OUTCOMES

- Increased coherence in HCC cells (τ doubles to ~ 8 –10 min).
- No change or decreased coherence.
- Selective effect on HCC vs. normal cells.
- Cytotoxicity at higher modulation intensities.

2.3 MOST PROBABLE OUTCOME

Partial restoration of coherence in HCC cells (τ increases by 20–50%, but not to normal levels), as biological systems often show incomplete stochastic resonance due to cellular heterogeneity and suboptimal noise parameters. Normal cells are likely unaffected or slightly disrupted, based on the known robustness of healthy signaling.

2.4 BRANCH 2.1: OPTIMIZE NOISE PARAMETERS

Trigger. Partial or no coherence restoration.

Approach. Systematically vary modulation parameters.

1. Test ranges: frequencies 0.01–2 Hz, amplitudes 0.5–1.5 mM CaCl_2 , durations 0.5–10 s, in a factorial design.

2. Repeat imaging and analysis; fit data to a resonance curve (coherence vs. noise intensity).
3. $n = 3$ replicates.

Resources. Additional HBSS formulations; curve-fitting software (GraphPad Prism).

Expected Outcomes. Optimal parameters identified; no optimum found; resonance in normal cells too.

Most Probable. Identification of a modest optimum (e.g., 0.1 Hz, 2 s pulses) with partial enhancement, as full resonance is rare in heterogeneous cell populations per biophysical precedents.

2.5 BRANCH 2.2: MEASURE DOWNSTREAM SIGNALING ACTIVATION

Trigger. Successful coherence restoration (increased $\tau > 20\%$).

Approach. Assess NF- κ B and NFAT activation.

1. Post-modulation, fix cells and immunostain with anti-p65 (NF- κ B, Cell Signaling, 1:200) and anti-NFAT (Abcam, 1:100). Quantify nuclear translocation via confocal imaging ($n = 100$ cells/group).
2. Perform qRT-PCR for downstream targets *p21* and *cyclin D*.
3. Include controls: TNF α (10 ng/ml) as NF- κ B positive control.

Resources. Antibodies as specified; qRT-PCR kit; TNF α (Sigma).

Expected Outcomes. Increased *p21*, decreased *cyclin D*; no change; or paradoxical activation.

Most Probable. Mild increase in *p21* (~ 1.5 -fold), but inconsistent *cyclin D* changes, reflecting partial signaling restoration amid cancer cell adaptations.

3 STEP 3: EVALUATE CELL CYCLE CHECKPOINT REGULATION AND PROLIFERATION EFFECTS

3.1 APPROACH

Rationale. This functional validation assesses if restored calcium coherence translates to re-engaged checkpoints and reduced proliferation in HCC cells, using flow cytometry and proliferation assays as standard, feasible methods to link signaling to phenotypic outcomes.

Procedure.

1. Subject HepG2 and normal cells to optimized noise modulation (from Step 2) for 24 h in the microfluidic setup.
2. Harvest and stain with propidium iodide (50 μ g/ml) for cell cycle analysis via flow cytometry (BD FACSCalibur); quantify G1/S/G2 fractions.
3. Perform parallel MTT assay (0.5 mg/ml, 4 h incubation) for proliferation, reading absorbance at 570 nm.
4. Include controls: no modulation, constant low calcium (0.8 mM), and doxorubicin (1 μ M) as positive antiproliferative control.
5. Conduct $n = 3$ independent experiments and analyze with ANOVA.

Required Resources.

- **Cell lines/models:** Same as previous steps, for consistency.
- **Key reagents:** Propidium iodide (Sigma, 50 μ g/ml); MTT kit (Promega); Doxorubicin (Sigma, 1 μ M).
- **Equipment:** Flow cytometer (BD FACSCalibur); spectrophotometer.

3.2 EXPECTED OUTCOMES

- G1 arrest and reduced proliferation in HCC cells.
- No effect on cell cycle or proliferation.
- Selective effect on HCC vs. normal.
- Induction of apoptosis.

3.3 MOST PROBABLE OUTCOME

Modest G1 accumulation ($\sim 10\text{--}20\%$ increase) and proliferation reduction ($\sim 30\%$) in HCC cells, but not complete arrest, as cancer cells often resist checkpoint restoration due to multiple mutations; normal cells unaffected, consistent with selective vulnerability.

4 INTEGRATION STRATEGY

STEP 1 provides baseline data essential for interpreting STEP 2 and STEP 3. Positive outcomes from STEP 2 (coherence restoration) feed into STEP 3 for functional validation, while branches allow mechanistic refinement. Together, they build evidence from characterization to mechanism to phenotype, with cross-validation (e.g., using the same cell models and imaging across steps).

5 CRITICAL DECISION POINTS

- If **STEP 1** shows no baseline differences, abandon hypothesis (no disruption to restore).
- If **STEP 2** fails to restore coherence even after optimization (Branch 2.1), conclude against stochastic resonance in this system.
- If **STEP 3** shows no proliferation effect despite signaling changes (Branch 2.2), hypothesis partially refuted (mechanism present but functionally irrelevant).

6 SUCCESS CRITERIA

Hypothesis validated if the following conditions are met:

- Baseline disruption confirmed ($\tau < 50\%$ of normal).
- Noise increases $\tau > 50\%$ in HCC selectively.
- $> 20\%$ G1 arrest and $> 40\%$ proliferation reduction in HCC, with statistical significance ($p < 0.01$) and validated controls.

7 CONTINGENCY PLANS

- If microfluidic modulation fails (e.g., cell detachment), switch to bulk perfusion in multi-well plates with manual media changes.
- If HepG2 lacks robust oscillations, substitute with Huh7 HCC line.
- For low signal-to-noise in imaging, use ratiometric dyes such as Fura-2.

8 RAW STATEMENT FROM SPACER

```

{
  "concept": "Controlled noise injection into calcium signaling pathways may restore
oscillatory coherence in hepatocellular carcinoma cells through stochastic resonance
mechanisms. This approach could potentially re-establish calcium-dependent cell cycle
checkpoint regulation that appears disrupted in malignant hepatocytes compared to
normal physiological fluctuation patterns.",
  "rationale": [
    {
      "statement": "Hepatocellular carcinoma cells exhibit fundamentally altered calcium
homeostasis and signaling dynamics compared to healthy hepatocytes. These cancer
cells show disrupted calcium oscillations, altered NFB signaling patterns,
decreased expression of plasma membrane Ca2+-ATPase leading to sustained high
intracellular calcium levels, and disrupted circadian rhythms that normally
coordinate calcium oscillations with cell cycle checkpoints.",
      "supporting_dois": [
        "10.1002/ijc.21591",
        "10.1002/jcb.1140",
        "10.1002/jnr.1120",
        "10.1002/mc.20446",
        "10.1016/j.apsb.2023.05.031",
        "10.1016/j.biomaterials.2022.121823",
        "10.1016/j.celrep.2017.10.099",
        "10.1038/s41419-019-1613-2",
        "10.1073/pnas.2214829120",
        "10.1073/pnas.75.12.6069",
        "10.1093/neuonc/noae165.0260",
        "10.1152/ajpcell.00181.2006",
        "10.1158/0008-5472.can-11-3782",
        "10.1158/0008-5472.can-16-1611",
        "10.1158/2159-8290.cd-rw2022-225",
        "10.1159/000111116",
        "10.1523/eneuro.0160-17.2017",
        "10.18632/oncotarget.11037",
        "10.18632/oncotarget.24352",
        "10.18632/oncotarget.5225",
        "10.3390/cancers11101588",
        "10.3390/ijms25115748",
        "10.54254/2753-8818/2024.1a19855"
      ]
    },
    {
      "statement": "Stochastic resonance represents a fundamental principle where
introducing optimal levels of noise enhances temporal coherence of weak periodic
signals in nonlinear systems. In biological contexts, controlled introduction of
specific noise patterns can amplify oscillatory coherence, and non-Gaussian noise
patterns have been demonstrated to optimize temporal patterns in calcium signaling
networks.",
      "supporting_dois": [
        "10.1007/s11433-008-0061-2",
        "10.1063/1.1697377",
        "10.1063/1.2920175",
        "10.1088/0256-307x/21/8/070",
        "10.1103/physreve.71.061916",
        "10.1142/s0218127410027994",
        "10.1142/s0219477511000363",
        "10.1142/s0219477512500083"
      ]
    },
    {
      "statement": "Hepatocyte calcium signaling networks possess the essential
nonlinear dynamics required for stochastic resonance effects. Theoretical models
demonstrate that intracellular calcium systems in sub-threshold, excitable states
can exhibit coherence resonance, where optimal noise levels enhance regularity of
intrinsic oscillations. These systems approximate real cell dimensions necessary
for meaningful stochastic resonance effects.",
      "supporting_dois": [
        "10.1002/cphc.200400089",
        "10.1007/s11433-008-0061-2",
        "10.1016/s1872-1508(08)60083-2",
        "10.1039/b501344e",
        "10.1063/1.2920175",
        "10.1088/0256-307x/21/8/070",
        "10.1088/1674-0068/21/06/521-525",
        "10.1088/1674-1056/18/3/005"
      ]
    }
  ]
}

```

```

324         "10.1103/physreve.71.061916",
325         "10.1103/physreve.74.031901",
326         "10.1142/s0218127410027994",
327         "10.1142/s0219477511000363",
328         "10.1142/s0219477512500083",
329         "10.7498/aps.58.7458"
330     ],
331     {
332         "statement": "Calcium oscillation coherence serves as a critical signaling code
333         that encodes information determining activation of specific downstream genetic
334         programs controlling cell cycle progression. The precise temporal patterns of
335         these oscillations are decoded by pathways that differentially activate
336         transcription factors like NF-B and NFAT, which regulate expression of key cell
337         cycle checkpoint proteins such as p21 and cyclin D.",
338         "supporting_dois": [
339             "10.1002/stem.1813",
340             "10.1016/j.molcel.2016.11.011",
341             "10.1038/s41598-022-10095-1",
342             "10.1073/pnas.1614613114",
343             "10.1074/jbc.274.48.33995",
344             "10.1074/jbc.m109.066704",
345             "10.1080/23723556.2014.1002714",
346             "10.1088/1478-3975/7/3/036009",
347             "10.1093/neuonc/noaa215.130",
348             "10.1093/neuonc/noad179.0098",
349             "10.1093/neuonc/noae165.0260",
350             "10.1096/fasebj.10.13.8940296",
351             "10.1126/science.1099962",
352             "10.1126/science.1164860",
353             "10.1128/mcb.19.4.2690",
354             "10.1139/o00-012",
355             "10.1152/ajpcel.00181.2006",
356             "10.1158/2159-8290.cd-rw2022-225",
357             "10.1242/jcs.082727"
358         ]
359     },
360     {
361         "statement": "Cancer cells demonstrate selective vulnerability to calcium-based
362         interventions due to their altered calcium handling mechanisms. Targeted
363         approaches can exploit differential calcium transport, sensing receptor
364         expression, and homeostasis between healthy and malignant cells to selectively
365         inhibit proliferation or induce calcium-mediated cell death pathways like
366         calciptosis.",
367         "supporting_dois": [
368             "10.1002/adhm.201900501",
369             "10.1002/adma.202310818",
370             "10.1002/ijc.27902",
371             "10.1016/j.bbamcr.2017.01.017",
372             "10.1039/d4ma00050a",
373             "10.1073/pnas.1413409111",
374             "10.1097/md.00000000000011095",
375             "10.1124/jpet.110.178194",
376             "10.1155/2012/512907",
377             "10.1158/1535-7163.mct-11-0965",
378             "10.18632/oncotarget.16999",
379             "10.2174/1381612829666230331084848",
380             "10.3389/fgene.2023.1215645",
381             "10.3390/biology13030168",
382             "10.3390/cancers15061825",
383             "10.3390/ijms221810124",
384             "10.3727/000000003108748072",
385             "10.3892/ijmm.2015.2167"
386         ]
387     },
388     {
389         "statement": "Controlled aperiodic modulation of extracellular calcium
390         concentrations provides a technologically feasible method to inject noise into
391         intracellular calcium signaling systems. Modulating extracellular calcium directly
392         influences intracellular oscillation dynamics by altering electrochemical
393         gradients and flux through ion channels and pumps, enabling systematic enhancement
394         of signal-to-noise ratios in endogenous oscillations.",
395         "supporting_dois": [
396             "10.1002/jcb.1140",
397             "10.1002/jcp.1040980105",
398             "10.1002/jcp.1041610202",
399             "10.1073/pnas.94.4.1194",
400             "10.1083/jcb.200402136",
401             "10.1152/ajpcel.1989.256.5.c951",

```

```

378         "10.1152/ajpcell.1991.261.1.c177",
379         "10.1161/01.res.0000223059.19250.91",
380         "10.1254/jjp.63.83"
381     ]
382 },
383 {
384     "statement": "The proposed experimental parameters for calcium modulation fall
385     within safe, physiologically relevant ranges for healthy hepatocytes while
386     effectively targeting cancer cell vulnerabilities. Extracellular concentrations of
387     0.8-1.25 mM, modulation frequencies of 0.05-1.0 Hz, and pulse durations of 1-5
388     seconds align with natural cellular signaling kinetics while avoiding cytotoxicity
389     in normal cells.",
390     "supporting_dois": [
391         "10.1002/hep.1840190521",
392         "10.1016/j.isci.2021.103139",
393         "10.1016/s0021-9258(17)35230-4",
394         "10.1016/s0021-9258(18)71469-5",
395         "10.1016/s0022-3565(25)22647-7",
396         "10.1016/s0026-895x(25)08805-4",
397         "10.1042/bj20021289",
398         "10.1042/bj2630347",
399         "10.1042/bj2680627",
400         "10.1042/bj2870645",
401         "10.1042/bj2910163",
402         "10.1042/bj3280573",
403         "10.1042/bj3301411",
404         "10.1042/bst0381247",
405         "10.1073/pnas.75.12.6069",
406         "10.1074/jbc.272.5.2675",
407         "10.1074/jbc.274.48.33995",
408         "10.1074/jbc.m009317200",
409         "10.1074/jbc.m115.713008",
410         "10.1074/jbc.m510085200",
411         "10.1074/jbc.m706831200",
412         "10.1085/jgp.109.5.571",
413         "10.1097/00006676-200611000-00074",
414         "10.1097/00007890-199902150-00019",
415         "10.1111/j.1469-7793.1997.00017.x",
416         "10.1111/j.1600-0676.1994.tb00074.x",
417         "10.1111/j.1749-6632.2000.tb05603.x",
418         "10.1126/science.1071914",
419         "10.1126/science.1099962",
420         "10.1126/science.1164860",
421         "10.1126/science.386513",
422         "10.1158/0008-5472.can-16-1611",
423         "10.1186/bcr1845",
424         "10.1186/s13046-018-0714-6",
425         "10.1242/jcs.069641",
426         "10.1242/jcs.082727",
427         "10.1371/journal.pcbi.1003965",
428         "10.2174/156800961506150805151905",
429         "10.3390/ijms15022672"
430     ]
431 },
432 {
433     "statement": "Advanced microfluidic technologies combined with sophisticated
434     live-cell imaging enable precise delivery of complex temporal noise patterns and
435     quantitative measurement of their effects. These systems provide the necessary
436     temporal resolution and spatial control to generate non-Gaussian noise patterns
437     while monitoring calcium oscillation coherence and cell cycle status in
438     real-time.",
439     "supporting_dois": [
440         "10.1002/bkcs.10521",
441         "10.1002/hep.1840160229",
442         "10.1002/jcp.1040980105",
443         "10.1016/s0021-9258(18)71469-5",
444         "10.1016/s0021-9258(18)87017-x",
445         "10.1021/ac202595g",
446         "10.1038/s41586-023-05828-9",
447         "10.1038/s41592-023-01852-9",
448         "10.1038/srep38276",
449         "10.1039/b313600k",
450         "10.1039/c41c00642a",
451         "10.1039/c41c01070a",
452         "10.1039/c6ib00186f",
453         "10.1039/c9ay01328h",
454         "10.1039/d01c00419g",
455         "10.1042/cbi20100643",
456         "10.1049/mnl:20065031",

```



```

    "10.1063/5.0109263",
    "10.1074/jbc.270.14.8102",
    "10.1088/1674-1056/22/1/010501",
    "10.1089/ten.tea.2018.0020",
    "10.1089/ten.tec.2018.0204",
    "10.1101/pdb.prot078642",
    "10.1101/pdb.prot080408",
    "10.1109/aim.2019.8868767",
    "10.1109/biophotonics.2015.7304038",
    "10.1109/robio.2004.1521794",
    "10.1109/tnb.2018.2882223",
    "10.1113/jp283832",
    "10.1117/12.580734",
    "10.1126/science.2011747",
    "10.1126/science.2154851",
    "10.1126/stke.2582004p115",
    "10.1142/s0218127410027994",
    "10.1142/s0219477512500083",
    "10.1152/ajpheart.1997.272.1.h236",
    "10.1152/jn.00679.2010",
    "10.1247/csf.16.341",
    "10.1260/1759-3093.1.1.27",
    "10.1371/journal.pone.0010237",
    "10.1371/journal.pone.0045917",
    "10.1371/journal.pone.0051286",
    "10.1371/journal.pone.0168342",
    "10.21769/bioprotoc.3504",
    "10.3389/fmed.2022.835700",
    "10.3390/e24030370",
    "10.3390/mil2020161",
    "10.3390/pr9010021"
  ]
},
{
  "statement": "Restoring physiological-like coherence to disrupted calcium
oscillations in cancer cells may re-engage homeostatic control mechanisms and
suppress malignant phenotypes. The transition from healthy to cancerous states
often involves loss of coherent signaling dynamics in favor of simplified,
persistent signaling states that promote proliferation. Therefore, re-imposing
coherent, physiological-like signal patterns could restore homeostatic regulatory
network function.",
  "supporting_dois": [
    "10.1103/physreve.80.030903",
    "10.1103/physrevlett.85.2833",
    "10.1126/science.aao3048",
    "10.1186/1752-0509-4-162",
    "10.2174/157436207780619545"
  ]
}
]
}

```

Figure 2: *Spacer's* output of *Restoring Calcium Oscillations in Hepatocellular Carcinoma* in STATEMENT format. The experimental procedures were generated by Grok 4 based on it.